Available online at www.sciencedirect.com
SCIENCE DIRECT®
Journal of Organometallic Chemistry 670 (2003) 221–234
Journal of Organometallic Chemistry
www.elsevier.com/locate/jorganchem

Synthesis, structures and photophysics of novel luminescent platinum–copper complexes

Irene Ara [a], Jesús R. Berenguer [b], Eduardo Eguizábal [b], Juan Forniés [a,*], Julio Gómez [b], Elena Lalinde [b,*]

[a] Departamento de Química Inorgánica, Instituto de Ciencia de Materiales de Aragón, Universidad de Zaragoza-Consejo Superior de Investigaciones Científicas, E-50009 Zaragoza, Spain
[b] Departamento de Química-Grupo de Síntesis Química de La Rioja, UA-CSIC, Universidad de La Rioja, E-26006 Logroño, Spain

Received 15 November 2002; received in revised form 20 December 2002; accepted 20 December 2002

Abstract

The novel hexanuclear platinum–copper complex $[Pt_2Cu_4(C_6F_5)_4(C{\equiv}C^tBu)_4(acetone)_2]$ (**1**) and the polynuclear derivative $[PtCu_2(C_6F_5)_2(C{\equiv}CPh)_2]_x$ (**2**), which crystallises in acetone as $[Pt_2Cu_4(C_6F_5)_4(C{\equiv}CPh)_4(acetone)_4]$ (**2**)·$(acetone)_4$, have been prepared using $[cis\text{-}Pt(C_6F_5)_2(THF)_2]$ and the corresponding copper–acetylide $[Cu(C{\equiv}CR)]_x$ (molar ratio 1:2) as starting materials. Treatment of **1** and **2** with 2,2′-bipyridine (molar ratio Cu–bipy 1:1), afforded the new trinuclear derivatives $[\{cis\text{-}Pt(C_6F_5)_2(\mu\text{-}C{\equiv}CR)_2\}\{Cu(bipy)\}_2]$ (R = ^{t}Bu **3**, Ph **4**), in which the dianionic 3-platina-1,4-diyne acts as a didentate bridging ligand to two different cationic Cu(bipy) units through η^2-side-on coordination of the alkynyl fragments. While similar treatment of **1** with dppe (Cu–dppe 1:1) yielded $[\{cis\text{-}Pt(C_6F_5)_2(\mu\text{-}C{\equiv}C^tBu)_2\}\{Cu(dppe)\}_2]$ (**5**), the analogous reaction of **2** with dppe afforded a mixture of complexes containing $[Pt(C_6F_5)(C{\equiv}CPh)(dppe)]$ as the main platinum compound. The crystal structures of **1**, **2**·$(acetone)_4$, **3** and **4** and the luminescent behaviour of all complexes have been determined. A comparison of the photoluminescent spectra of **1** and **2** with those of the related platinum–silver species $[PtAg_2(C_6F_5)_2(C{\equiv}CR)_2]_x$ and the monomeric $[cis\text{-}Pt(C_6F_5)_2(C{\equiv}CR)_2]^{2-}$ suggests the presence of emitting states bearing a large cluster $[PtM_2]_x$-to-ligand (alkynide) charge transfer (CLCT).

Keywords: Platinum; Copper; Cluster; Alkynyl; Luminescence

1. Introduction

The synthesis and design of rigid-rod metal acetylide materials, as well as polynuclear containing multisite bound acetylide ligands, have attracted considerable attention [1], especially due to the potential application of these systems in non-linear optics [2], luminescence [3] and molecular conductivity [4]. The chemistry of alkynyl copper, in particular, has received much recent attention [5]. This has been partly due to the fact that discrete mono and polynuclear Cu(I) alkynyl species have been shown to exhibit a rich photochemistry and they belong to a kind of luminophores that may have applications in electronic devices [3a,6]. Copper–alkynyl has also been widely employed in organic transformations and is a key step, not only in many palladium-catalysed homo and cross coupling alkyne reactions [7], but also in the preparation of a large number of metal σ-alkynide complexes [8]. So far, most of the studies in this latter synthetic methodology have been focused on ML_xX (X = halide)–RC≡CH systems with the presence of a catalytic amount of CuI and base. The reactions involve intermediate alkynylcopper(I) compounds, which undergo intermolecular exchange of the alkynyl and halide ligands [7a,7b,8a]. The final transmetallation is believed to occur via a bimetallic (M–Cu) intermediate stabilised through an alkynyl or an alkynyl–halide bridging system. These bonding situations are well exemplified by numerous reports on the use of alkynyl complexes, $L_nM(C{\equiv}CR)_x$, as η^2-alkyne ligands towards copper ions, yielding stable polymetallic aggregates with diverse and interesting structures [6c,9]. This versatile field has

* Corresponding authors.
E-mail addresses: juan.fornies@posta.unizar.es (J. Forniés), elena.lalinde@dq.unirioja.es (E. Lalinde).

0022-328X/03/$ - see front matter © 2003 Elsevier Science B.V. All rights reserved.
doi:10.1016/S0022-328X(03)00012-3

been comprehensively reviewed by Lang et al. [10]. In addition, recent studies have established that the nature of metal···copper and alkynyl···copper bonding interactions play a key role in the final photophysical and photochemical properties of these systems [3,6]. In view of the potential interest of these final heteropolynuclear species, it is rather surprising that relatively limited work has been carried out to investigate the reactivity of polymeric $[Cu(C{\equiv}CR)]_n$ derivatives with unsaturated organometallic compounds or containing labile solvent ligands.

Some years ago, we reported the synthesis and structural properties of several alkynyl bridged oligomeric heteropolynuclear platinum–silver systems, obtained by reaction of the insoluble polymeric species $[Ag(C{\equiv}CR)]_n$ with platinum substrates [11]. In these reactions, the silver–acetylide acts as an alkynylating agent displacing labile coordinated ligands, the resulting platinate species being stabilised by silver–η^2-acetylide and weak Pt–Ag bonding interactions. At this point, we became interested in finding out whether acetylide–copper species behave similarly, and also in gaining further insights into the spectroscopic and luminescence properties of the final heteropolynuclear platinum–copper and platinum–silver complexes.

In this paper, we report the reactivity of the solvate complex [*cis*-$Pt(C_6F_5)_2(THF)_2$] towards $[Cu(C{\equiv}CR)]_x$ (R = ^{t}Bu, Ph), which has allowed us to carry out the synthesis of two unusual hexanuclear solvate clusters $[Pt_2Cu_4(C_6F_5)_4(C{\equiv}C^tBu)_4(acetone)_2]$ (**1**) and $[Pt_2Cu_4(C_6F_5)_4(C{\equiv}CPh)_4(acetone)_4]$ (**2**)·(acetone)$_4$, and a second class of trinuclear $PtCu_2$ derivatives [{*cis*-$Pt(C_6F_5)_2(\mu\text{-}C{\equiv}CR)_2$}{Cu(bipy)}$_2$] (R = ^{t}Bu **3**, Ph **4**) and [{*cis*-$Pt(C_6F_5)_2(\mu\text{-}C{\equiv}C^tBu)_2$}{Cu(dppe)}$_2$] (**5**), respectively, generated using **1** and **2** as precursors. In addition, the study of the photoluminescence properties of all Pt–Cu complexes (**1**–**5**), and a comparison with the properties of the analogous platinum–silver cluster species previously reported $[PtAg_2(C_6F_5)_2(C{\equiv}CR)_2]$ (R = ^{t}Bu **6**, Ph **7**) [11b], are also included.

2. Results and discussion

2.1. Hexanuclear Pt_2Cu_4 clusters

Treatment of [*cis*-$Pt(C_6F_5)_2(THF)_2$] with a yellow suspension of $[Cu(C{\equiv}C^tBu)]_x$ in acetone (molar ratio Pt:Cu 1:2.5) produces, after removal of the excess of $[Cu(C{\equiv}C^tBu)]_x$, a yellow solution, from which a pale yellow microcrystalline solid of stoichiometry $[PtCu_2(C_6F_5)_2(C{\equiv}C^tBu)_2(acetone)]_2$ (**1**) is obtained by evaporation of the solvent and addition of diethylether (Scheme 1). The isolation of a pure complex in the analogous [*cis*-$Pt(C_6F_5)_2(THF)_2$]–$[Cu(C{\equiv}CPh)]_x$ system requires the treatment of the final yellow residue with chloroform. Under these preparative conditions, a bright orange solid of the expected stoichiometry $[PtCu_2(C_6F_5)_2(C{\equiv}CPh)_2]$ (**2**) separates. This orange solid **2** is insoluble in non-coordinated solvents such as $CHCl_3$, CH_2Cl_2 or *n*-hexane, but it is soluble in donor solvents such as diethylether, acetone or tetrahydrofuran. The slow diffusion of *n*-hexane into a yellow solution of **2** in acetone produces a yellow microcrystalline solid, identified by X-ray crystallography as the solvate cluster **2**·(acetone)$_4$. This microcrystalline solid looses solvent quickly reverting to the initial deep-orange material **2**.

Both complexes **1** and **2** have been characterised by usual spectroscopic (IR, ^{19}F-, ^{1}H- and ^{13}C-NMR) and spectrometric (mass) techniques. In addition, the dimeric nature of **1** and **2**·(acetone)$_4$ has been confirmed by X-ray crystallography. Crystals of **1** have been obtained by slow diffusion of *n*-hexane into a solution of **1** in a mixture of acetone and diethylether (5:1), and its molecular structure (Fig. 1, Table 1) confirms that double alkynylation of the platinum atoms has taken place, giving rise to dianionic bis(alkynyl)platinate fragments, which are neutralised by four copper atoms through η^2-alkyne interactions (Fig. 1a). Complex **1** $[Pt_2Cu_4(C_6F_5)_4(C{\equiv}C^tBu)_4(acetone)_2]$ is a very unusual hexanuclear Pt_2Cu_4 species, which is formed by a distorted planar tetranuclear cationic entity $[Cu_4(acetone)_2]^{+4}$ capped by two $[Pt(C_6F_5)_2(C{\equiv}C^tBu)_2]^{2-}$ anions. It is remarkable that the analogous platinum–silver derivative $[PtAg_2(C_6F_5)_2(C{\equiv}C^tBu)_2]$ (**6**) dissolves in acetone, yielding a tetrasolvate hexanuclear species of stoichiometry $[Pt_2Ag_4(C_6F_5)_4(C{\equiv}C^tBu)_4(acetone)_4]$ (see Scheme 1), which looses acetone when it is air dried. The structure of this cluster [11b], **6**·(acetone)$_4$, is very different, being formed by two identical {*cis*-$Pt(C_6F_5)_2(\mu\text{-}C{\equiv}C^tBu)_2Ag(acetone)_2$} units linked by two bridging Ag(I) ions through additional η^2-Ag linkages.

To our surprise, the structure of **1** contains two different dimetallatetrahedrane Cu_2C_2 units. As can be observed in Fig. 1b, which shows a view of the central framework, while one of the 3-platinadiyne fragments, C(8)–C(7)–[Pt(1)]–C(1)–C(2), is building up both Cu_2C_2 tetrahedrons, the alkynyl fragments of the other platinum unit, C(14)–C(13)–[Pt(2)]–C(19)–C(20), complete, together with the solvent (acetone) molecules, the coordination environments of the copper centres. Two short distances (Cu(1)–Cu(3) 2.5839(8); Cu(2)–Cu(4) 2.6106(8) Å) and two long distances (Cu(1)–Cu(4) 2.8610(8), Cu(2)–Cu(3) 2.8355(8) Å) are found within the central framework. The former are comparable with those reported for related dimetallatetrahedrane systems [9b], and close to the separation found in metallic copper (2.56 Å), suggesting at least weak Cu(I)···Cu(I) contacts. The remaining Cu···Cu separations are longer than the sum of the van der Waals radii for two Cu(I) atoms (2.8 Å) [12], excluding Cu(I)···Cu(I) interactions

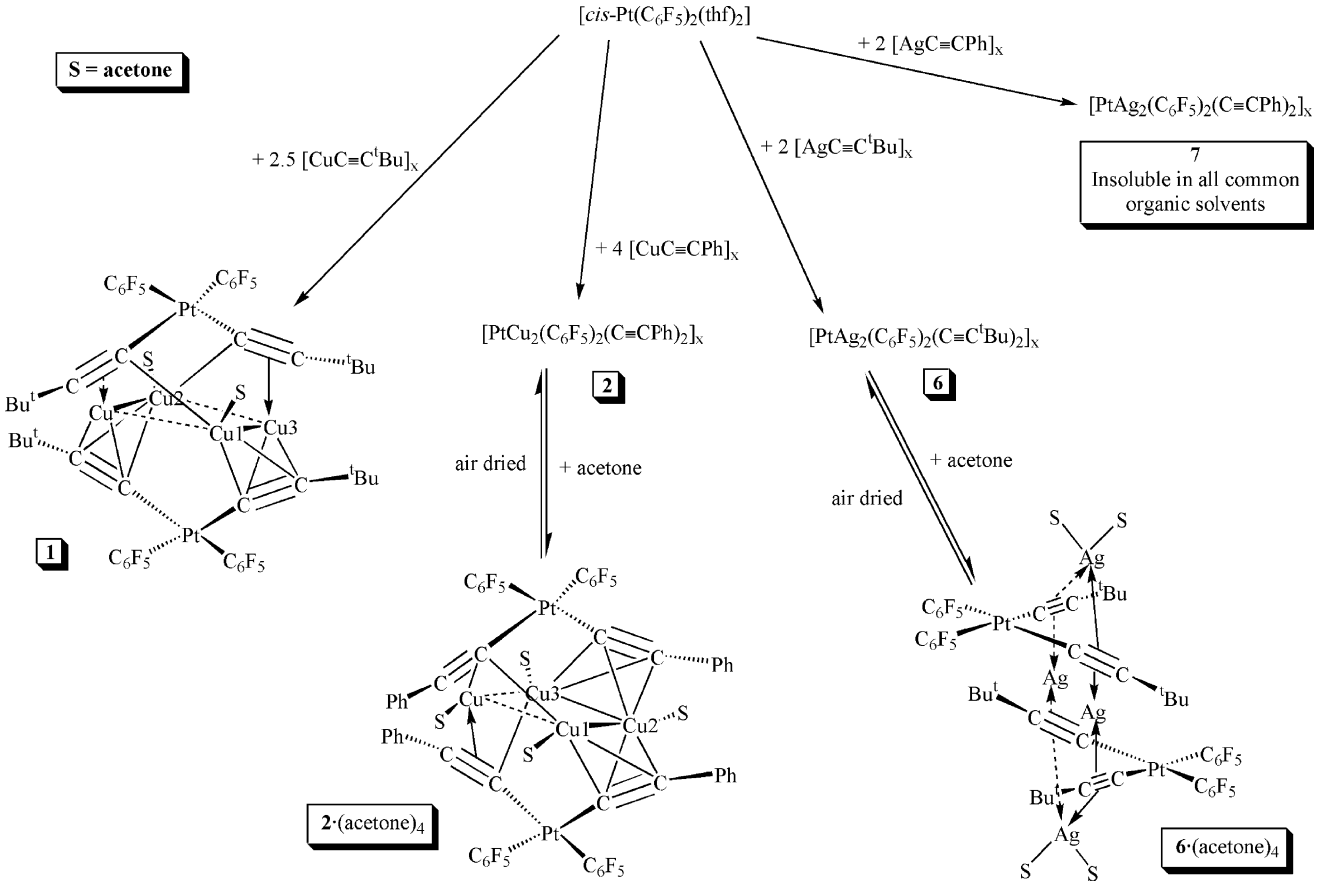

Scheme 1.

between both dimetallatetrahedrons. The Pt···Cu distances, falling in the range from 2.9449(7) for Pt(1)–Cu(3) to 3.777 Å for Pt(1)–Cu(2), are larger than those found in related alkynyl platinum–copper clusters: $[Pt_2Cu_4(C{\equiv}CPh)_8]_n$ ($n = 2$ [13], 3 [6c]; range 2.918(1)–3.027(1) Å), $[(1,1\text{-ferrocenyldiyl})Pt_2Cu_3(C{\equiv}CPh)_6]$ (2.845(5)–2.975(3) Å) [14] or $[(PEt_3)Cp^*Rh(\mu\text{-}C{\equiv}CPh)_2Cu_2(\mu\text{-}C{\equiv}CPh)_2Pt(C_6F_5)_2]$ (2.9226(14), 2.9384(13) Å) [15], excluding the existence of Pt···Cu bonding interactions. The four copper atoms are not coplanar, but the angle between the Cu(1)–Cu(3) and Cu(2)–Cu(4) vectors is only 18.8°. However, the two 3-platinadiyne ligands are nearly perpendicular, the dihedral angle being formed by the best platinum coordination planes 79.91°.

In each Cu_2C_2 unit, one of the copper centres (Cu(3) and Cu(4)) is linearly bonded (excluding the Cu···Cu interaction) to two alkynyl fragments; while the other (Cu(1) and Cu(3)) has a nearly trigonal-planar coordination, being bonded to two alkynyl entities (one associated to each platinum unit) and to the oxygen atom of one acetone molecule (Cu(1)–O(1) 2.026(4) Å; Cu(2)–O(2) 2.026(4) Å). The Cu–C(alkyne) carbon distances are unexceptional ranging from 1.955(4) for Cu(3)–C(1) to 2.241(5) Å for Cu(3)–C(2). The bonding of copper centres Cu(1) and Cu(2) to the C_β carbon atoms, C(14) and C(20), respectively, seems to be very weak (Cu(1)–C(14) 2.259(4) Å; Cu(2)–C(20) 2.348(5) Å), probably due to the additional interaction of these atoms with one molecule of acetone. Consequently, while both alkynyl fragments of the Pt(1) unit are acting as μ^3-η^1(Pt):η^2(Cu): η^2(Cu) bridging ligands, the other two alkynyl groups associated to Pt(2) atom act as μ_3-η^1(Pt):η^1(Cu):η^2(Cu) ligands. Although the bite angle of both 3-platinadiyne ligands are similar (C(7)–Pt(1)–C(1) 104.44(17)°; C(13)–Pt(2)–C(19) 102.40(16)°), the dissimilarity in the alkynyl bonding mode is clearly reflected in the distortion from linearity of these ligands. The bend back angles at C_α and C_β carbons average 17.8 and 26.6°, respectively, in the C(8)–C(7)–[Pt(1)]–C(1)–C(2) unit, in comparison to only 10 and 17°, respectively, in the second C(14)–C(13)–[Pt(2)]–C(19)–C(20) unit.

In contrast to the previously reported platinum–silver $[PtAg_2(C_6F_5)_2(C{\equiv}CPh)_2]$ (**7**) [11b], which is insoluble in all common organic solvents (see Scheme 1), the orange platinum–copper–phenylethynyl derivative **2** dissolves in donor solvents (acetone, THF) giving yellow solutions. As noted above, slow diffusion, at low temperature, of *n*-hexane into a solution of **2** in acetone afforded the **2**·(acetone)$_4$ as yellow crystals. The single-crystal analysis revealed, as is shown in Fig. 2, Table 2, that the

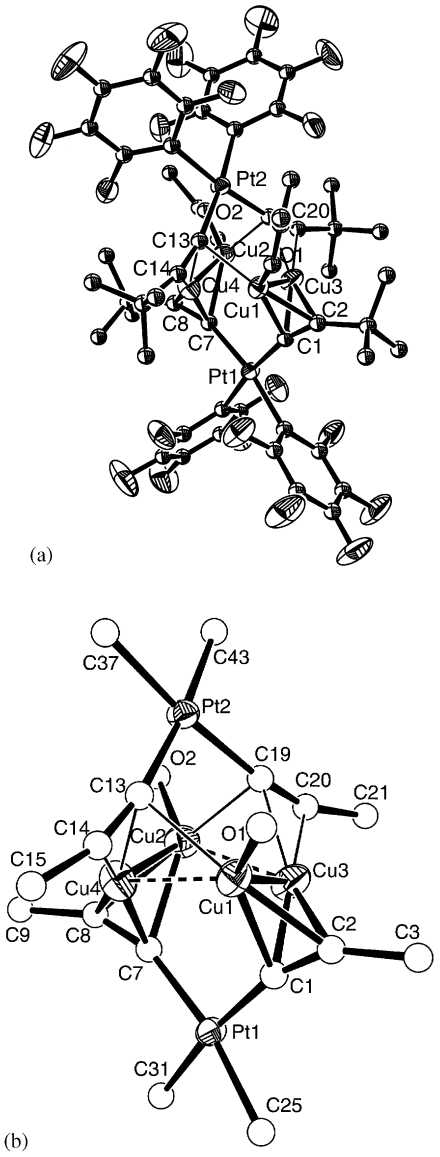

Fig. 1. (a) Molecular structure of $[Pt_2Cu_4(C_6F_5)_4(C{\equiv}C^tBu)_4(acetone)_2]\cdot 3H_2O$ (**1**·$3H_2O$) with the solvate and hydrogen atoms omitted. (b) Schematic view of the hexametallic central core of **1**·$3H_2O$.

Table 1
Selected bond lengths (Å) and angles (°) for complex $[Pt_2Cu_4(C_6F_5)_4(C{\equiv}C^tBu)_4(acetone)_2]\cdot 3H_2O$ (**1**)·$3H_2O$

Bond lengths			
Pt(1)–C(1)	2.032(5)	Cu(4)–C(14)	2.113(5)
Pt(1)–C(31)	2.054(4)	C(7)–C(8)	1.255(6)
Pt(2)–C(37)	2.057(4)	C(14)–C(15)	1.501(6)
Cu(1)–C(2)	2.041(3)	Pt(1)–Cu(1)	3.764
Cu(1)–C(14)	2.259(4)	Pt(1)–Cu(4)	3.1039(6)
Cu(2)–C(8)	2.064(4)	Pt(2)–Cu(3)	3.418
Cu(3)–C(1)	1.955(4)	Cu(1)–Cu(3)	2.5839(8)
Cu(3)–C(2)	2.241(5)	Cu(2)–Cu(4)	2.6106(8)
Cu(4)–C(13)	1.993(4)	Pt(1)–C(25)	2.048(4)
C(2)–C(3)	1.517(7)	Pt(2)–C(19)	2.032(4)
C(13)–C(14)	1.245(6)	Cu(1)–O(1)	2.026(4)
C(20)–C(21)	1.482(6)	Cu(1)–C(13)	2.184(4)
Pt(1)–Cu(3)	2.9449(7)	Cu(2)–C(7)	2.151(4)
Pt(2)–Cu(2)	3.170	Cu(2)–C(20)	2.348(5)
Cu(1)–Cu(2)	4.504	Cu(3)–C(20)	2.056(4)
Cu(2)–Cu(3)	2.8355(8)	Cu(4)–C(8)	2.151(5)
Pt(1)–C(7)	2.018(4)	C(1)–C(2)	1.248(6)
Pt(2)–C(13)	2.047(4)	C(8)–C(9)	1.508(6)
Pt(2)–C(43)	2.048(4)	C(19)–C(20)	1.233(6)
Cu(1)–C(1)	2.146(4)	Pt(1)–Cu(2)	3.777
Cu(2)–O(2)	2.026(4)	Pt(2)–Cu(1)	3.544
Cu(2)–C(19)	2.159(5)	Pt(2)–Cu(4)	3.0474(6)
Cu(3)–C(19)	2.030(4)	Cu(1)–Cu(4)	2.8610(8)
Cu(4)–C(7)	1.990(4)	Cu(3)–Cu(4)	2.9702(9)
Bond angles			
C(1)–Pt(1)–C(7)	104.44(17)	C(1)–Pt(1)–C(25)	83.95(17)
C(7)–Pt(1)–C(31)	82.59(17)	C(25)–Pt(1)–C(31)	89.23(17)
C(13)–Pt(2)–C(19)	102.40(16)	C(19)–Pt(2)–C(43)	83.36(17)
C(13)–Pt(2)–C(37)	85.78(17)	C(37)–Pt(2)–C(43)	88.48(18)
O(1)–Cu(1)–C(13)	101.92(16)	O(1)–Cu(1)–C(1,2)	123.57
C(1,2)–Cu(1)–C(13)	133.24	O(2)–Cu(2)–C(19)	105.61(16)
O(2)–Cu(2)–C(7,8)	124.53	C(7,8)–Cu(2)–C(19)	127.06
C(1,2)–Cu(3)–C(19,20)	167.32	C(7,8)–Cu(4)–C(13,14)	176.33
Pt(1)–C(1)–C(2)	163.2(4)	C(1)–C(2)–C(3)	152.7(4)
Pt(1)–C(7)–C(8)	161.2(4)	C(7)–C(8)–C(9)	154.2(4)
Pt(2)–C(13)–C(14)	168.3(4)	C(13)–C(14)–C(15)	163.9(4)
Pt(2)–C(19)–C(20)	171.8(4)	C(19)–C(20)–C(21)	161.8(5)

hexanuclear complex is formed by an essentially planar tetracopper unit (maximum deviation 0.032 Å for Cu(2)) capped again by two nearly orthogonal dianionic 3-platinadiyne ligands (dihedral angle 87.36°). In contrast to complex **1**, each copper bears an acetone molecule. Again, two short and two long Cu···Cu contacts are observed; in this case, two consecutive edges of the Cu_4 unit are shorter (Cu(1)–Cu(2) 2.7272(12) Å; Cu(2)–Cu(3) 2.6279(12) Å) than the other two (Cu(3)–Cu(4) 3.086 Å; Cu(1)–Cu(4) 3.532 Å). All copper atoms have a trigonal arrangement, being bonded to two alkynyl units (one associated to each Pt) and to one oxygen atom (Cu–O 1.999(6)–2.074(7) Å). As can be seen in Fig. 2b, in each platinum–diyne unit only one of the alkynyl entities is acting as a μ^3-η^1(Pt):η^2(Cu):η^2(Cu) bridging ligand, forming part of a dimetallatetrahedrane entity Cu_2C_2 (Cu–$C_{\alpha,\beta}$ 2.017(6)–2.178(6) Å), and, as a result, it is very distorted at C_β carbon (C(1)–C(2)–C(3) 154.5(7)°, C(17)–C(18)–C(19) 156.5(7)°). The C(25)≡C(26) alkynyl fragment at Pt(2) acts mainly as a μ^3-η^1(Pt):η^1(Cu):η^2(Cu) group, while the C(9)≡C(10) entity of Pt(1) clearly acts as a μ^3–η^1 ligand. Consequently, a C(9)–C(10)–C(11) angle of 174.0(8)°, which is close to linearity, is observed. The differences in the alkynyl bonding mode may arise from intramolecular steric overcrowding and irregularity in the Cu···Cu and Pt···Cu distances. Thus, the shortest Pt···Cu separations found [Pt(1)–Cu(1) 3.0866(9) Å and Pt(1)–Cu(4) 2.8924(9) Å] are associated with the μ^3–η^1 bonding ligand. The bite angle of both distorted 3-platinadiyne units (C(1)–Pt(1)–C(9) 102.7(3)°; C(17)–Pt(2)–C(25) 103.5(3)°) is similar to those observed in **1**.

Table 2
Selected bond lengths (Å) and angles (°) for complex $[Pt_2Cu_4(C_6F_5)_4(C{\equiv}CPh)_4]\cdot(acetone)_4$ (**2**)·(acetone)$_4$

Bond lengths			
Pt(1)–C(1)	2.027(6)	Cu(4)–C(10)	2.304(7)
Pt(1)–C(39)	2.046(7)	C(1)–C(2)	1.255(9)
Pt(2)–C(45)	2.046(7)	C(10)–C(11)	1.429(10)
Cu(1)–C(9)	2.050(7)	C(25)–C(26)	1.282(9)
Cu(1)–C(18)	2.017(6)	Pt(1)–Cu(2)	3.701
Cu(2)–C(2)	2.040(6)	Pt(2)–Cu(1)	3.651
Cu(3)–O(3)	2.039(5)	Pt(2)–Cu(4)	3.494
Cu(3)–C(25)	2.092(6)	Cu(1)–Cu(4)	3.532
Cu(4)–C(9)	2.076(7)	Cu(3)–Cu(4)	3.086
Cu(4)–C(26)	2.020(6)	Pt(1)–C(33)	2.045(7)
C(9)–C(10)	1.233(9)	Pt(2)–C(25)	1.998(8)
C(18)–C(19)	1.454(9)	Cu(1)–O(1)	1.999(6)
Pt(1)–Cu(1)	3.0866(9)	Cu(1)–C(17)	2.065(7)
Pt(1)–Cu(4)	2.8924(9)	Cu(2)–C(1)	2.108(6)
Pt(2)–Cu(3)	3.262	Cu(2)–C(18)	2.178(6)
Cu(1)–Cu(3)	4.099	Cu(3)–C(2)	2.037(6)
Cu(2)–Cu(4)	4.313	Cu(4)–O(4)	2.068(5)
Pt(1)–C(9)	2.041(7)	Cu(4)–C(25)	2.066(7)
Pt(2)–C(17)	2.009(7)	C(2)–C(3)	1.479(9)
Pt(2)–C(51a)	2.077(8)	C(17)–C(18)	1.262(9)
Cu(1)–C(10)	2.501(7)	C(26)–C(27)	1.431(9)
Cu(2)–O(2)	2.074(7)	Pt(1)–Cu(3)	3.499
Cu(2)–C(17)	2.144(6)	Pt(2)–Cu(2)	3.410
Cu(3)–C(1)	2.085(6)	Cu(1)–Cu(2)	2.7272(12)
Cu(3)–C(26)	2.282(6)	Cu(2)–Cu(3)	2.6279(12)
Bond angles			
C(1)–Pt(1)–C(9)	102.7(3)	C(9)–Pt(1)–C(39)	84.5(3)
C(1)–Pt(1)–C(33)	85.2(3)	C(39)–Pt(1)–C(33)	87.6(3)
C(17)–Pt(2)–C(25)	103.5(3)	C(25)–Pt(2)–C(45)	81.3(3)
C(17)–Pt(2)–C(51a)	82.8(3)	C(45)–Pt(2)–C(51a)	93.0(3)
O(1)–Cu(1)–C(9)	101.6(3)	O(1)–Cu(1)–C(17,18)	126.95
C(17,18)–Cu(1)–C(9)	131.42	O(2)–Cu(2)–C(17,18)	99.44
O(2)–Cu(2)–C(1,2)	121.93	C(1,2)–Cu(2)–C(17,18)	138.49
O(3)–Cu(3)–C(1,2)	125.56	C(25)–Cu(3)–C(1,2)	130.99
O(3)–Cu(3)–C(25)	101.9(2)	O(4)–Cu(4)–C(9)	104.0(2)
O(4)–Cu(4)–C(25,26)	124.22	C(9)–Cu(4)–C(25,26)	131.81
Pt(1)–C(1)–C(2)	162.3(5)	C(1)–C(2)–C(3)	154.5(7)
Pt(1)–C(9)–C(10)	166.0(6)	C(9)–C(10)–C(11)	174.0(8)
Pt(2)–C(17)–C(18)	162.1(6)	C(17)–C(18)–C(19)	156.5(7)
Pt(2)–C(25)–C(26)	167.7(5)	C(25)–C(26)–C(27)	157.8(7)

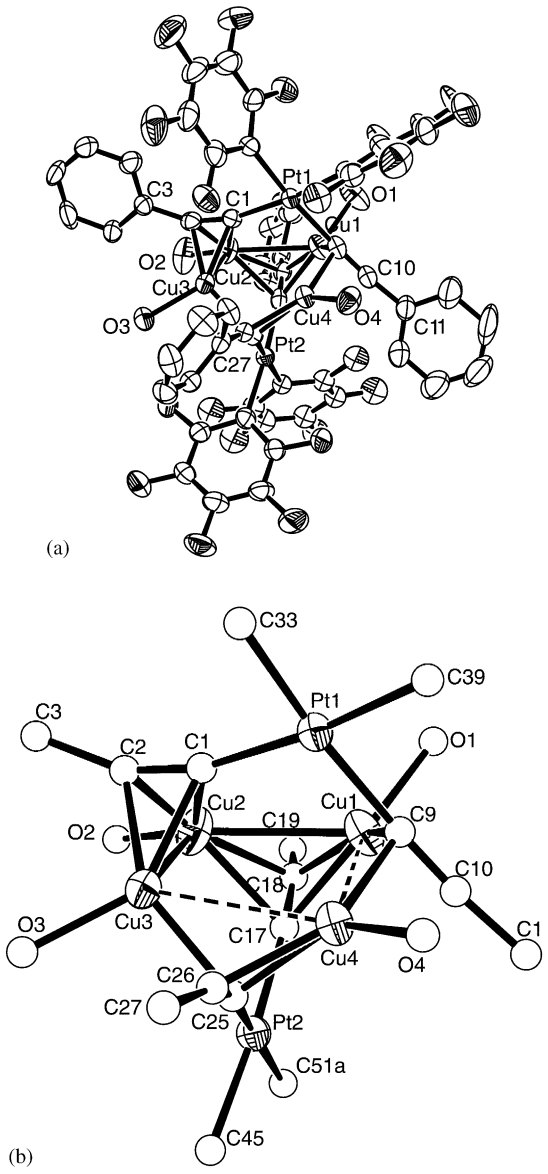

Fig. 2. (a) Structure of $[Pt_2Cu_4(C_6F_5)_4(C{\equiv}CPh)_4]\cdot(acetone)_4$ (**2**)·(acetone)$_4$. The carbon atoms of the acetone ligand and the hydrogen atoms have been omitted for clarity. (b) Schematic view of the hexametallic central core of **2**·(acetone)$_4$.

The structures of **1** and **2**·(acetone)$_4$ suggest that the unsolvate material **2** presumably has a similar structure based on a tetranuclear Cu_4 unit, probably with short Cu···Cu contacts, capped by two orthogonal $[cis\text{-}Pt(C_6F_5)_2(C{\equiv}CPh)_2]^{2-}$ fragments through η^2···Cu alkyne bonding interactions. In solution, acetone or THF donor solvents probably interact with the copper centres, causing a weakening of Cu–alkyne and/or Cu···Cu interactions of **2**. However, the real nuclearity of these platinum–copper species in solution is uncertain. The electrospray mass spectra of both complexes (**1**, **2** EI^-) display the corresponding monomeric anion $[PtCu(C_6F_5)_2(C{\equiv}CR)_2]^-$ (*m*/*z* 755 R = ^{t}Bu **1**; 795 R = Ph **2**) as the parent molecular ion, and molecular peaks whose isotopic distributions agree with the expected dimeric formulation with the loss of a Cu ion $[Pt_2Cu_3(C_6F_5)_4(C{\equiv}CR)_4]^-$ (*m*/*z* 1573 (44%) R = ^{t}Bu **1**; 1653 (65%) R = Ph **2**). Although this fact clearly supports the existence in solution of hexanuclear species similar to those found for **1** or **2**·(acetone)$_4$ in the solid state, the presence of higher oligomeric species can not be discarded. Thus, we noted that in the FAB^- mass spectrum of **1**, in addition to the dimeric fragment at *m*/*z* 1573, a peak at *m*/*z* 2392 (25%) attributable to a trimeric anion $[Pt_3Cu_5(C_6F_5)_6(C{\equiv}C^tBu)_6]^-$ is also observed.

The IR (Nujol) and ^{13}C-NMR ($CDCl_3$ **1** and CD_3COCD_3 **2**) spectra of both complexes are consistent

with a η^2-coordination of Cu(I) ions to the alkynyl groups. Particularly significant is the appearance of $\nu_{C\equiv C}$ absorptions (1988(w) cm^{-1} **1**; 1989, 1964, 1952(sh) cm^{-1} **2**), which are shifted to lower frequencies when compared with those of the corresponding anionic [*cis*-$Pt(C_6F_5)_2(C\equiv CR)_2]^{2-}$ species (R = ^{t}Bu 2085, 2090 cm^{-1}. R = Ph 2095, 2082 cm^{-1}) [16a]. The coordinated C_α and C_β alkynyl carbon resonances appears at δ 89.9 and 132.9 in **1** and at δ 113.7 and 101.4 in **2**. When these signals are compared with those observed in [*cis*-$Pt(C_6F_5)_2(C\equiv CR)_2]^{2-}$ (R = ^{t}Bu δ 98.2 C_α, 110.13 C_β; [16b] R = Ph δ 117.1 C_α, 102.4 C_β) a notable shift to high-field is found for the C_α carbon resonances in both complexes. In contrast to this, the acetylenic C_β resonance clearly moves downfield in **1** and slightly upfield in **2**. For complex **2**, the appearance of small additional carbon signals due to the aromatic C_6H_5 groups in the ^{13}C-NMR spectrum at low temperature (−50 °C, see Section 4) suggests the presence of at least two different species in solution. The proton and ^{19}F-NMR spectra of complex **2** also confirms this fact, which is particularly obvious in the ^{19}F-NMR spectrum. At room temperature, the ^{19}F-NMR spectrum of **2** is similar to that observed for **1**, displaying only one characteristic set of three 19-fluorine signals (2*o*-F, *p*-F, 2*m*-F), thus showing that all C_6F_5 are equivalent and indicating an effective equivalence of the two *o*-F and two *m*-F nuclei (AA′MXX′ system). Upon cooling the pattern of these three fluorine resonances does not experience a significant change, but a new small set of additional signals merges from the baseline, indicating the presence of some other species in low concentration, that are probably in rapid equilibrium at higher temperatures. In the proton spectrum of **1**, in addition to a singlet due to ^{t}Bu groups (δ 1.17) and the expected resonances attributed to bound CH_3COCH_3 molecules (δ 2.32), a broad singlet occurs at δ 2.26. We attribute this signal to H_2O molecules present in the $CDCl_3$ solvent, which coordinate to two of the copper(I) centres, replacing the acetone molecules to some extent. This signal shifts considerably to low-field (δ 3.90) when the solution is cooled to 233 K.

2.2. Trinuclear $PtCu_2$ complexes

The solvent molecules and some of the η^2-alkyne interactions are easily removed from the copper ion's coordination sphere in complexes **1** and **2**. In particular, the reactivity of **1** and **2** towards 2,2′-bipy and 1,2-bis(diphenylphosphine)ethane (dppe) has been investigated (Scheme 2). Addition of four equivalents of 2,2′-bipyridine (Pt:bipy 1:2) to a yellow solution of **1** in CH_2Cl_2 or **2** in acetone yields orange (**1**) or deep yellow (**2**) solutions, from which neutral trinuclear alkynyl bridged complexes [{*cis*-$Pt(C_6F_5)_2(\mu$-$C\equiv CR)_2$}{Cu(bipy)}$_2$] (R = ^{t}Bu **3**, Ph **4**) are isolated as orange (**3**) or yellow (**4**) microcrystalline solids in good yields. An analogous trinuclear complex [{*cis*-$Pt(C_6F_5)_2(\mu$-$C\equiv C^tBu)_2$}{Cu(dppe)}$_2$] (**5**) is obtained as a white solid by reaction of **1** with four equivalents of dppe. However, the reaction of **2** with dppe (Pt:dppe 1:2) immediately produces a mixture of complexes in which the platinum mononuclear complex [$Pt(C_6F_5)$(C≡CPh)(dppe)] (δ^{31}P 43.45, $^1J_{PtP}$ 2342 Hz; 38.29, $^1J_{PtP}$ 2232 P *trans* to C_6F_5) and other copper–phosphine (δ^{31} P −9.41(br); δ^{31} P −16.5(br)) derivatives are clearly detected.

In contrast to complexes **3** and **4**, which are stable in the solid state and in solution, complex **5** is air-stable in the solid state, but decomposes slowly in solution yielding, as the main platinum complex (^{31}P- and ^{19}F-NMR), the mononuclear derivative [$Pt(C_6F_5)$(C≡C^tBu)(dppe)] (δ^{31} P 43.48, $^1J_{PtP}$ 2310 Hz; 37.38, $^1J_{PtP}$ 2266 (m, P *trans* to C_6F_5)).

The formulation given in Scheme 2 for complexes **3**–**5** is based on spectroscopic data and confirmed by X-ray diffraction studies of complexes **3** and **4**, respectively. The molecules are shown in Figs. 3 and 4, and relevant distances and angles are given in Table 3.

As can be observed, in both molecules the dialkynyl–platinate entity acts as a bridging bidentate ligand to two cationic Cu(bipy)$^+$ units. Both molecules exhibit an approximately square-planar coordination environment around the platinum centre, made up of two C_6F_5 ligands mutually *cis* and two alkynyl groups. As expected, the Pt–C_α (C_{sp}) distances (1.973(4)–2.008(3) Å) are slightly shorter than the corresponding Pt–C_{ipso} (C_{sp^2}) (2.039(4)–2.052(3) Å), and essentially similar to those found in other heterobimetallic complexes [15,16] containing this type of dianionic $[Pt(C_6F_5)_2(C\equiv CR)_2]^{2-}$ fragment. The bite C_α–Pt–C_α angles (89.74(13)° **3**, 87.2(2)° **4**) are smaller than those observed for **1** and **2**·(acetone)$_4$, but comparable with those observed in other heterobimetallic complexes, in which similar 3-platina-1,4-diine fragments [Pt](C≡CR)$_2$ act as bridging or even as chelating bidentate ligands [16,17].

The geometry of the copper atoms is essentially trigonal-planar; each copper atom is bonded to two nitrogen atoms of the bipy ligand and η^2-bonded to one alkyne moiety of the dialkynyl platinum entity. The sum of bond angles within the CuN_2C_2 moieties is ca. 360°. This trigonal-planar arrangement has many precedents in acetylide bridged and copper(I)–alkyne complexes [10]. The Cu–N distances (1.986(3)–2.083(2) Å) compare well with those observed in the heteropolynuclear copper cation $[Cu_5(C\equiv C^tBu)_2(bipy)_4]^{3+}$ (2.017–2.093 Å) [18] or in other related alkyne mononuclear copper–diimine derivatives [19].

The copper–alkyne carbon bond distances are symmetrical (Cu–C_α 1.980(4)–2.012(3) Å and Cu–C_β 1.956(4)–2.049(3) Å), and typical of copper–η^2-alkyne structures [10]. Though the parameters for the acetylenic units (C≡C distances and angles at C_α and C_β) are

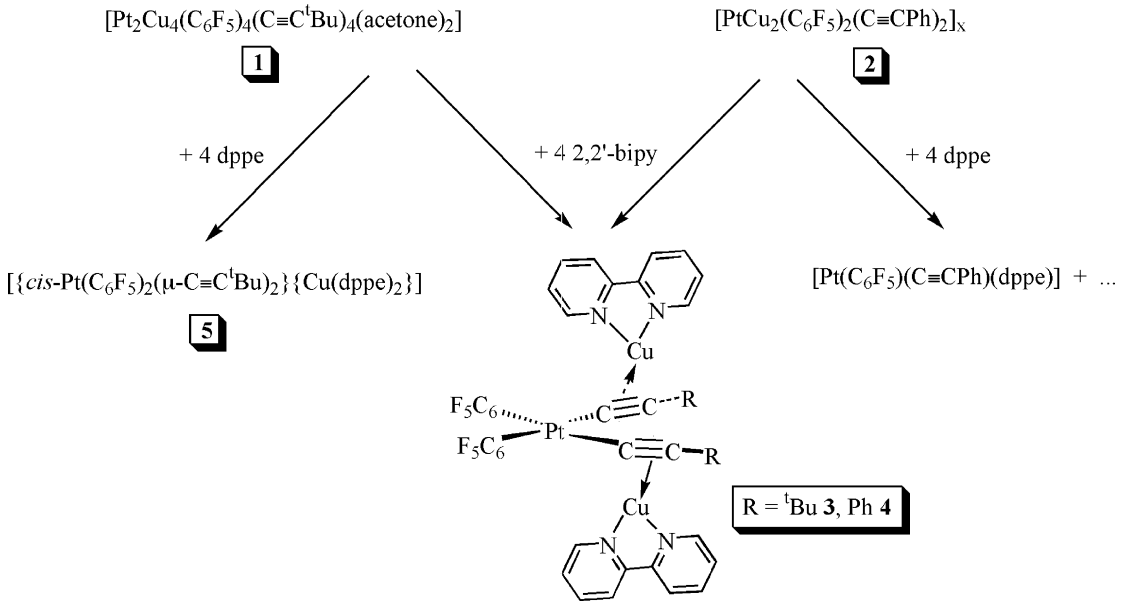

Scheme 2.

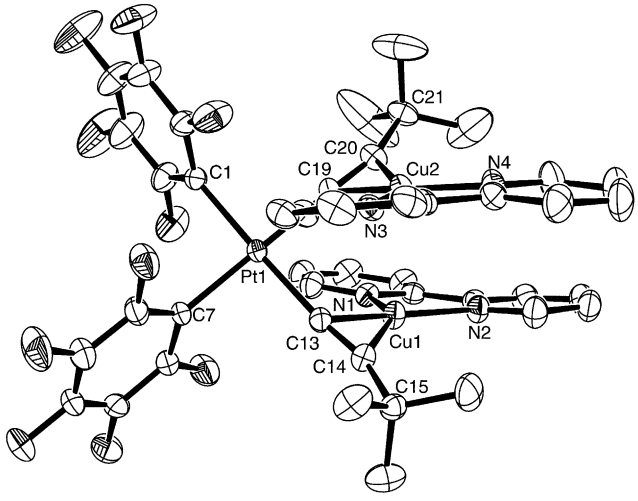

Fig. 3. Molecular structure of [{*cis*-Pt(C_6F_5)$_2$(μ-C≡C^{t}Bu)$_2$}{Cu(bipy)}$_2$] (**3**) with the hydrogen atoms omitted.

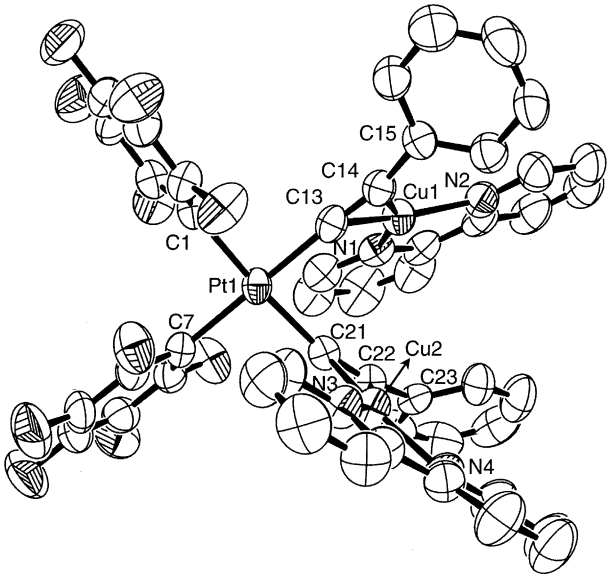

Fig. 4. Structure of [{*cis*-Pt(C_6F_5)$_2$(μ-C≡CPh)$_2$}{Cu(bipy)}$_2$]·acetone (**4**·acetone) with the solvate and hydrogen atoms omitted.

unexceptional, coming within the normal range for σ, π bonding modes, it is worth noting that the symmetrical side-bonding interaction causes a slightly more marked bending at C_β (154.9(3)–159.7(4)°) than at C_α (165.6(4)–172.7(2)°).

The most remarkable and distinct feature of both structures is found in the relative orientation of both Cu(bipy) units with respect to the platinum coordination plane. Thus, in complex **3** the copper centres, and their corresponding bipy ligands, are proximally located with regard to the *cis* C(19)–Pt(1)–C(13) angle formed by their respective acetylide ligands. The copper-containing units, however, have a mutual *anti*-disposition with respect to the platinum coordination plane, giving the molecule an overall two-fold rotation axis, which bisects the C(19)–Pt(1)–C(13) angle. The dihedral angles between the Pt coordination plane and the corresponding copper coordination planes (Cu, N, N and the midpoint of C≡C) are 59.69° for Cu(I) and 59.60° for Cu(2). As a consequence, the copper coordination planes are nearly parallel, forming an angle of only 5.81°, and the Cu···Cu separation (3.153 Å) is shorter than that found in **4**. In the phenyletynyl derivative compound **4**, one of the Cu(bipy)$^+$ units [Cu(2)(bipy)] lies on a plane which is nearly perpendicular to the Pt coordination plane (dihedral angle 86.02°). The other

Table 3
Selected bond lengths (Å) and angles (°) for complexes [{*cis*-Pt(C_6F_5)$_2$(μ-1κC^{α}:η^2-C≡C^{t}Bu)$_2$}{Cu(bipy)}$_2$] (**3**) and [{*cis*-Pt(C_6F_5)$_2$-(μ-1κC^{α}:η^2-C≡CPh)$_2$}{Cu(bipy)}$_2$]·acetone (**4**·acetone)

3			
Bond lengths			
Pt(1)–C(1)	2.050(3)	Cu(2)–N(3)	2.047(2)
Pt(1)–C(19)	2.008(3)	C(19)–C(20)	1.249(4)
Cu(1)–N(1)	2.083(2)	Pt(1)–Cu(1)	3.270
Cu(2)–C(20)	2.008(3)	Pt(1)–C(13)	1.998(3)
C(13)–C(14)	1.251(4)	Cu(1)–C(14)	2.049(3)
Cu(2)–C(19,20)	1.910	Cu(2)–C(19)	2.012(3)
Cu(1)–Cu(2)	3.153	Cu(2)–N(4)	2.031(3)
Pt(1)–C(7)	2.052(3)	Cu(1)–C(13,14)	1.927
Cu(1)–C(13)	2.004(3)	Pt(1)–Cu(2)	3.369
Cu(1)–N(2)	2.017(3)		
Bond angles			
C(1)–Pt(1)–C(7)	91.62(12)	C(1)–Pt(1)–C(19)	88.48(13)
C(7)–Pt(1)–C(13)	90.19(12)	C(19)–Pt(1)–C(13)	89.74(13)
C(13)–Cu(1)–C(14)	35.93(11)	C(19)–Cu(2)–C(20)	36.22(13)
N(1)–Cu(1)–N(2)	80.19(11)	N(3)–Cu(2)–N(4)	80.72(11)
C(14)–C(13)–Pt(1)	169.2(3)	C(20)–C(19)–Pt(1)	172.7(3)
C(13)–C(14)–C(15)	154.9(3)	C(19)–C(20)–C(21)	155.7(3)
N(1)–Cu(1)–C(13,14)	129.67	N(2)–Cu(1)–C(13,14)	149.48
N(3)–Cu(2)–C(19,20)	129.76	N(4)–Cu(2)–C(19,20)	148.79
4·*acetone*			
Bond lengths			
Pt(1)–C(1)	2.039(4)	Cu(2)–N(3)	1.986(3)
Pt(1)–C(21)	1.992(4)	C(21)–C(22)	1.223(5)
Cu(1)–N(1)	1.996(3)	Pt(1)–Cu(1)	3.398
Cu(2)–C(22)	1.956(4)	Pt(1)–C(13)	1.973(4)
C(13)–C(14)	1.222(5)	Cu(1)–C(14)	1.961(4)
Cu(2)–C(21,22)	1.871	Cu(2)–C(21)	1.980(4)
Cu(1)–Cu(2)	4.306	Cu(2)–N(4)	2.000(4)
Pt(1)–C(7)	2.047(4)	Cu(1)–C(13,14)	1.890
Cu(1)–C(13)	2.011(4)	Pt(1)–Cu(2)	3.416
Cu(1)–N(2)	2.019(4)		
Bond angles			
C(13)–Pt(1)–C(21)	87.2(2)	C(1)–Pt(1)–C(7)	91.3(2)
C(7)–Pt(1)–C(21)	92.9(2)	C(13)–Pt(1)–C(1)	88.6(2)
C(13)–Cu(1)–C(14)	35.8(2)	C(21)–Cu(2)–C(22)	36.2(2)
N(1)–Cu(1)–N(2)	81.0(2)	N(3)–Cu(2)–N(4)	81.0(2)
C(14)–C(13)–Pt(1)	171.0(4)	C(22)–C(21)–Pt(1)	165.6(4)
C(13)–C(14)–C(15)	159.4(4)	C(21)–C(22)–C(23)	159.7(4)
N(2)–Cu(1)–C(13,14)	141.93	N(1)–Cu(1)–C(13,14)	137.08
N(3)–Cu(2)–C(21,22)	138.44	N(4)–Cu(2)–C(21,22)	140.55

copper containing unit is tilted proximally in relation to the *cis* C(acetylide)–Pt–C(acetylide) angle, and reveals a dihedral angle of 56.82° in relation to the Pt coordination plane. The copper coordination planes form an angle of 61.22° and the Cu···Cu separation is very long (4.306 Å). The Pt···Cu distances, slightly shorter in **3** than in **4**, are out of the van der Waals limits (3.15 Å).

In agreement with the structures shown in the Scheme 2, the IR spectra show the $\nu_{C\equiv C}$ absorptions in the expected region for bridging alkynyl ligands (1934 **3**, 1930 **4**, 2002 cm^{-1} **5**). In particular, the notable $\Delta\nu_{C\equiv C}$ shift in relation to the anionic [*cis*-Pt(C≡CR)$_2$(C_6F_5)$_2$]$^{2-}$ substrates [16a] (average ~154 **3**; 159 **4**, 86 cm^{-1} **5**) suggests a strong copper–η^2-alkyne bonding interaction. In addition to a collection of peaks due to bipy ligands, the ^{13}C-NMR spectrum of the most soluble complex **3** exhibits two broad signals at δ 116.1 and 97.0, which are assigned to C_β and C_α acetylide carbon atoms. The proton and ^{19}F-NMR spectra clearly indicate that these complexes are involved in dynamic processes. Only one type of C_6F_5 ligand, which displays the typical AA′MXX′ pattern, is observed in the ^{19}F-NMR spectra, thus indicating that the platinum coordination plane is a mirror plane. In addition, the ^{1}H-NMR spectra of **3** and **4** (four different aromatic protons for the bipy ligand) and the ^{31}P{^{1}H}-NMR spectra of **5** (δ_P 6.55) indicate the existence of a dynamic process which averages both halves of the bipyridine and dppe ligands. At first sight, the equivalencies observed at room temperature could be explained by assuming that the rotation of C_6F_5 groups around their Pt–*i*-C bonds and those of Cu(L–L) fragments around the corresponding Cu–alkyne bonds are fast on the NMR time scale. Alternatively, a simple associative mechanism involving fast coordination and decoordination of the Cu(L–L) fragments to both alkynyl entities, via four-coordinate copper intermediates type **B** (Scheme 3), is also likely. In order to obtain some insight into the behaviour of these species in solution, variable temperature NMR spectra were conducted for **3** and **4**. When the solutions of **3** and **4** are cooled to 213 K the four signals, due to the bipy ligand in the proton spectra, broaden but only the H33′ protons decoalesce into two broad singlets. Unfortunately, in both complexes, the low frequency resonance overlaps with other signals (H55′ protons for **3** and H66′ protons for **4**), and its correct position can not be assigned unambiguously even carrying out low temperature ^{1}H–^{1}H phase-sensitive NOESY experiments. Thus, only approximate values of $\Delta\nu$ and $\Delta G^{\#}$ can be obtained (for **3**, $\Delta\nu$ ~975 Hz, T_c ~223 K, $\Delta G^{\#}$ ~39.7 kJ·mol^{-1}. For **4**, $\Delta\nu$ ~1020 Hz, T_c ~223 K, $\Delta G^{\#}$ ~39.6 kJ·mol^{-1}). Below 218 K the *ortho*-fluorine atoms also become non-equivalent in the phenylethynyl derivative complex **4**, being observed as two different signals at 218 K. However, for **3** decoalescence of the *oo*′-F signal could not be achieved, even by cooling at 213 K. At this temperature only the broadening of the signal is evident, indicating a significant barrier to site exchange of the halves of C_6F_5. For complex **4**, the $\Delta G^{\#}_{218}$ value for the fluorine exchange at the coalescence temperature was 39.9 kJ·mol^{-1}. This value is notably smaller to those reported for the rotation of C_6F_5 groups in platinum and palladium square-planar complexes [20], and is similar to that found for the exchange of the bipy halves. This led us to conclude that, in this complex, an associative mechanism, such as that depicted in Scheme 3, which equilibrates both ends of the bipy ligands,

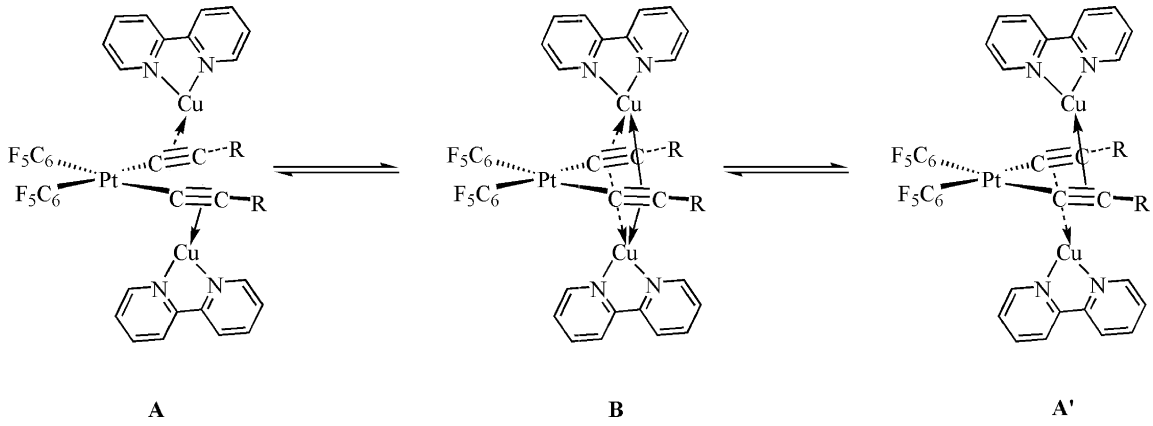

Scheme 3.

could be also responsible for the observed platinum mirror plane.

3. Photophysical properties

As has already been pointed out, this type of multimetallic system is often brightly luminescent even at room temperature, and with an emissive behaviour, which varies considerably with the structure and environment. In particular, the presence of short metal···metal contacts is believed to play a remarkable role in the excited-state properties. Along these lines, the trinuclear complexes **3** and **4**, containing the Cu(I)–bipy moieties and very long Pt···Cu or Cu···Cu distances, are not emissive in solution (CH_2Cl_2), nor in solid state (r.t. or 77 K).

The photophysical data for **1**, **2** and **5** are shown in Table 4, along with the data for the analogous platinum–silver phenylethynyl derivative $[PtAg_2(C_6F_5)_2(C{\equiv}CPh)_2]_n$ (**7**) [11b]. Data for the mononuclear $(PPh_3Me)_2[cis\text{-}Pt(C_6F_5)_2(C{\equiv}CPh)_2]$ and $(NBu_4)_2[cis\text{-}Pt(C_6F_5)_2(C{\equiv}C^tBu)_2]$ are also included for comparison. The analogous tertbutyl derivative $[PtAg_2(C_6F_5)_2(C{\equiv}C^tBu)_2]$ (**6**) does not show luminescent behaviour.

The mononuclear dianionic platinum complexes are slightly emissive in the solid state at room temperature. The phenyl derivative $(PPh_3Me)_2[cis\text{-}Pt(C_6F_5)_2(C{\equiv}CPh)_2]$ exhibits a vibronic structural band at λ_{max}^{em} 441, 459, 481 nm (λ_{max}^{exc} 341 nm); while for the *tert*-butyl compound $(NBu_4)_2[cis\text{-}Pt(C_6F_5)_2(C{\equiv}C^tBu)_2]$ only a weak emission is detected at 360 nm upon excitation in the range 240–260 nm. On the basis of previous studies on alkynyl platinum complexes 9a, [21] and the large Stokes-shifts, these emissions are attributed to alkynyl $^3(\pi\rightarrow\pi^*)$ excited states, with an admixture of a phenyl and acetylenic character in the phenylacetylide derivative.

The luminescence of the hexanuclear complex $[Pt_2Cu_4(C_6F_5)_4(C{\equiv}C^tBu)_4(acetone)_2]$ (**1**) is quite temperature dependent. This behaviour has many precedents in polynuclear Cu(I) compounds [22]. As can be observed in Fig. 5, the room temperature emission spectrum of **1** in CH_2Cl_2 displays a low energy band at 637 nm (λ_{exc} 402 nm), which is shifted remarkably (ca. 3030 cm^{-1}) by lowering the temperature to 77 K. It is interesting to note that at room temperature the solid (KBr) emission and excitation spectra are similar to those observed in fluid solution (λ_{max}^{em} 620 nm, λ_{exc} 424 nm), suggesting a similar origin. As has been noted above, the related yellow-pale platinum–silver(I) derivative $[PtAg_2(C_6F_5)_2(C{\equiv}C^tBu)_2]$ (**6**) is not emissive. This behaviour is not unexpected, and could be tentatively attributed to the presence of weaker Ag(I)···Ag(I) and Ag(I)···alkyne bonding interactions compared with those found in **1** (Ag···Ag 3.039(2) Å; Ag(I)–alkyne 2.221(9)–2.856(9) Å in **6**·(acetone)$_4$ vs. Cu···Cu 2.5839(8)–2.9702(9) Å; Cu(I)–alkyne 1.955(4)–2.241(5) Å in **1**). In agreement with this, the insoluble and probably polymeric phenylethynyl complex $[PtAg_2(C_6F_5)_2(C{\equiv}CPh)_2]_n$ (**7**), which has a deeper yellow colour and probably stronger Pt···Ag and Ag···Ag bonding interactions, also displays a broad emission centred at 588 nm.

The platinum–copper compound $[PtCu_2(C_6F_5)_2(C{\equiv}CPh)_2]_x$ (**2**) is also luminescent in solid state. Excitation of a KBr pellet of **2** (Fig. 6) at 465 nm gave a broad emission band (λ 642 nm), with a shoulder at lower energies. Upon excitation to lower energies (λ_{exc} 537 nm), the low energy shoulder is clearly enhanced and becomes dominant with a maximum at 787 nm by exciting at 635 nm, indicating dual-emission nature. Similarly, excitation of **5** at 365 nm gives a broad emission centred at 530 nm and with $\lambda_{exc} = 395$ nm at ca. 527 and 566 nm, respectively.

The red shift observed in the emission bands for all complexes in relation to the platinum mononuclear species suggests that orbitals involving Pt···M, M···M and M···alkynyl (M = Ag, Cu) interactions are likely to play a role in the excited states. Although one problem

Table 4
Emission and excitation spectral data for **1**–**7**

Compound	Medium (temperature K)	λ_{max}^{em} (nm)	λ_{max}^{exc} (nm)
$[Pt_2Cu_4(C_6F_5)_4(C{\equiv}C^tBu)_4(acetone)_2]$ (**1**)	KBr, (298)	620	424
	$CHCl_3$, 10^{-3} M (77)	534	331, 355
	$CHCl_3$, 10^{-3} M (298)	637	402
	Acetone, 10^{-3} M (77)	556	327, 358, 386
$[PtCu_2(C_6F_5)_2(C{\equiv}CPh)_2]_x$ (**2**)	Solid state, KBr (298)	642 [a]	399, 464, 540 [b]
		787 [c]	469, 580, 630 [d]
	Solid state, (298)	654	394, 468, 492, 535
	Solid state, (77)	664	395, 473, 487
[{*cis*-$Pt(C_6F_5)_2(\mu$-$C{\equiv}C^tBu)_2$}{Cu(dppe)}$_2$] (**5**)	Solid state, KBr (298)	530 [e]	384 [f]
		527, 566 [g]	393 [h]
	$CHCl_3$, 10^{-3} M (77)	500	343
	$CHCl_3$, 10^{-3} M (298)	401, 541	364
$[PtAg_2(C_6F_5)_2(C{\equiv}CPh)_2]_x$ (**7**)	Solid state, KBr (298)	588	389, 404, 468
$(NBu_4)_2$[*cis*-$Pt(C_6F_5)_2(C{\equiv}C^tBu)_2$]	Solid state, KBr (298)	360	210, 235, 240, 261
$(PMePh_3)_2$[*cis*-$Pt(C_6F_5)_2(C{\equiv}CPh)_2$]	Solid state, KBr (298)	441, 459, 481	341

[a] $\lambda_{exc} = 465$ nm.
[b] $\lambda_{emi} = 650$ nm.
[c] $\lambda_{exc} = 635$ nm.
[d] $\lambda_{emi} = 800$ nm.
[e] $\lambda_{exc} = 365$ nm.
[f] $\lambda_{emi} = 527$ nm.
[g] $\lambda_{exc} = 395$ nm.
[h] $\lambda_{emi} = 570$ nm.

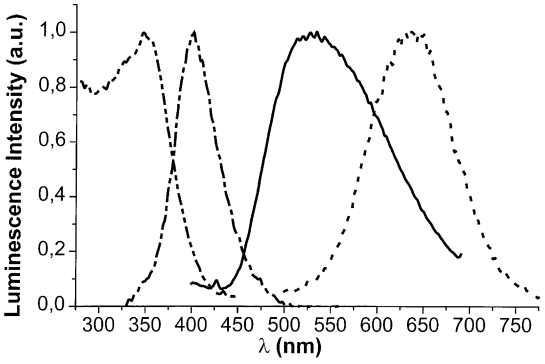

Fig. 5. Excitation (–·–· r.t.; –··–·· 77K) and emission (····· r.t.; — 77K) spectra of a solution 10^{-3} M of complex **1** in CH_2Cl_2.

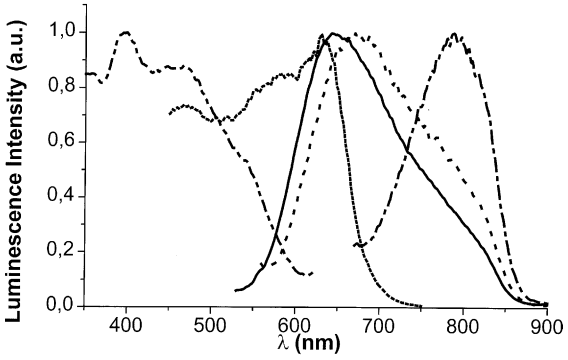

Fig. 6. Photoexcitation spectra monitoring the emission at 650 nm (–·· ·–··) and at 800 nm (·····) and emission spectra by exciting at 465 nm (—), at 537 nm (·····) and at 635 nm (–·–·) of a KBr pellet of complex **2** at room temperature.

in trying to compare spectra of complexes **1**, **2** and **7** is that changes in the metal coinage and in the alkynyl are probably accompanied by structural differences, the observation of that the emission band of the ^{t}Bu derivative **1** is blue shifted compared with **2** would suggest the involvement of the π*-C≡CR orbitals in the LUMO. As has been previously found [6b,9b] in other polynuclear clusters containing Cu(I) or Ag(I), the platinum–silver compound **7** shows a higher energy emission than the platinum–copper(I) derivative **2**. This fact could be related to stronger copper–alkyne bonding ($\nu_{C\equiv C}$ 1989, 1964, 1951 cm^{-1} in **2** vs. 2028 cm^{-1} in **7**), which probably lowers the LUMO energy, resulting in a narrower HOMO–LUMO gap. We tentatively assign the emissions to excited states with a substantial cluster $[PtM_2]_x$-to-ligand(π*-C≡CR) character (CLCT). The origin of the emission in complex **5** is more uncertain and participation of dppe ligands can not be excluded. Clearly, more detailed theoretical and new related systems are necessary to provide an insight into the origin of the emissions.

4. Experimental

4.1. General procedures and materials

All reactions were performed under a nitrogen atmosphere using standard Schlenk techniques. Solvents were purified according to standard procedures. NMR spectra were recorded on a Bruker ARX-300 spectrometer

and the $^1H-^1H$ phase-sensitive NOESY spectra was recorded following literature methods [23]. Chemical shifts are reported in ppm relative to external standards ($SiMe_4$, $CFCl_3$ and 85% H_3PO_4) and all coupling constants are given in Hz. IR spectra were obtained on Perkin–Elmer 883 or Perkin–Elmer FTIR Spectrum 1000 spectrometers using Nujol mulls between polyethylene sheets. Elemental analyses were carried out with a Perkin–Elmer 2400 CHNS/O or a Carlo Erba EA1110 CHNS-O microanalysers. Mass spectra were recorded on a VG Autospec double-focusing mass spectrometer operating in the FAB mode or a HP-5989B mass spectrometer using the ES techniques. Luminescence as well as excitation spectra were recorded in a Perkin–Elmer Luminescence Spectrometer LS 50B with a red sensitive R928 type photomultiplier. Literature methods were followed to prepare $[Cu(C{\equiv}CR)]_n$ (R = ^{t}Bu, Ph) [24] and [*cis*-$Pt(C_6F_5)_2(THF)_2$] [25].

4.2. Preparation of $[Pt_2Cu_4(C_6F_5)_4(C{\equiv}C^tBu)_4(acetone)_2]$ (1)

$[Cu(C{\equiv}C^tBu)]_n$ (0.13 g, 0.93 mmol) was added to an acetone (30 cm^3) solution of [*cis*-$Pt(C_6F_5)_2(THF)_2$] (0.25 g, 0.37 mmol), and the mixture was stirred at room temperature (r.t.) for 30 min. The final yellow suspension was filtered yielding a yellow solution, which was evaporated to dryness. Addition of Et_2O affords **1** as a yellow pale solid. Yield: 58% (0.19 g). Anal. Calc. For $C_{54}H_{48}O_2F_{20}Cu_4Pt_2$: C, 36.99; H, 2.76. Found: C, 37.26; H, 2.68%. ES^- (selected data): 1573 ($[Pt_2Cu_3(C_6F_5)_4(C{\equiv}C^tBu)_4]^-$, 44); 755 ($[PtCu(C_6F_5)_2(C{\equiv}C^tBu)_2]^-$, 100). FAB^- (selected data): 2392 ($[Pt_3Cu_5(C_6F_5)_6(C{\equiv}C^tBu)_6]^-$, 25); 1573 (6). IR($cm^{-1}$): 1988 w (C≡C), 798 vs, 790 vs $(C_6F_5)_{x\text{-sens}}$. ^1H-NMR ($CDCl_3$): At 293 K, 2.32 (s, $CH_3{-}CO{-}CH_3$), 2.26 (s br, probably due to coordinated H_2O which replaces acetone in some extent), 1.17 (s br, $C(C\underline{H}_3)_3$). Upon cooling, the signal observed at δ 2.26 shifts considerably to high frequency (δ 3.90 at −40 °C). ^{19}F-NMR ($CDCl_3$): At 293 K, −116.87 (d, $^3J_{PtF} = 399$, *o*-F), −161.6 (t, *p*-F), −164.3 (m, *m*-F). The same pattern is observed at low temperature. ^{13}C-NMR ($CDCl_3$): At 223 K, 207.1 (s, C=O, acetone), 146.3 (dm, $J_{FC} \sim 230$, C_6F_5), 136.4 (dm, $J_{CF} \sim 270$, C_6F_5), 89.9 ($C_\alpha{\equiv}$), 132.9 ($\equiv C_\beta$) (^{195}Pt satellites not observed), 34.35 (s, $\underline{C}(CH_3)_3$), 32.8 (s, CH_3, acetone), 31.4 (s, $C(\underline{C}H_3)_3$).

4.3. Preparation of $[PtCu_2(C_6F_5)_2(C{\equiv}CPh)_2]$ (2)

$[Cu(C{\equiv}CPh)]_n$ (0.15 g, 0.89 mmol) was added to a solution of [*cis*-$Pt(C_6F_5)_2(THF)_2$] (0.15g, 0.22 mmol) in acetone (40 cm^3), and the mixture was stirred at r.t. for 6 h. Excess $[Cu(C{\equiv}CPh)]_n$ was filtered through Kieselghur, and the resulting yellow solution evaporated to dryness. The final residue was treated with $CHCl_3$ to give **2** as an orange solid. Yield: 63% (0.12 g). Anal. Calc. For $C_{28}H_{10}F_{10}Cu_2Pt$: C, 39.17; H, 1.17. Found: C, 38.94; H, 0.90%. ES^- (selected data): 1653 ($[Pt_2Cu_3(C_6F_5)_4(C{\equiv}CPh)_4]^-$, 65); 795 ($[PtCu(C_6F_5)_2(C{\equiv}C^tBu)_2]^-$, 100). FAB^- (selected data): 1713 ($[Pt_2Cu_4(C_6F_5)_4(C{\equiv}C^tBu)_4{-}3]^-$, 4). IR($cm^{-1}$): 1989 br, 1964 br, 1951 sh (C≡C), 802 s br $(C_6F_5)_{x\text{-sens}}$. ^1H-NMR (CD_3COCD_3): At 293 K, 7.30, 7.12 (ArH). At 223 K a new small signal at δ 7,45 is also observed. ^{19}F-NMR (CD_3COCD_3): At 293 K, −115.2 (d, $^3J_{PtF} = 384$, *o*-F), −164.7 (t, *p*-F), −165.97 (m, *m*-F). At 223 K two different species are observed in a ca. ratio 3:1 (Majority species: −115.1 (d, $^3J_{PtF} = 386$, *o*-F), −164.67 (t, *p*-F), −165.38 (m, *m*-F). Minority species: −115.64 (d, $^3J_{PtF} = 380$, *o*-F), −165.18 (t, *p*-F), −165.89 (m, *m*-F)). ^{13}C-NMR (CD_3COCD_3): At 223 K, 148.2 (dm, $J_{FC} \sim 230$, C_6F_5), 136.6 (dm, $J_{CF} \sim 240$, C_6F_5), 132.2 (majority species), 132.0, 129.2, 129.05 (majority species), 128.9, 128.3, 126.1, 125.3 (majority species), 113.7 (s, C≡C), 101.4 (s, C≡C).

4.4. Preparation of $[\{cis\text{-}Pt(C_6F_5)_2(\mu\text{-}C{\equiv}CR)_2\}\{Cu(bipy)\}_2]$ (R = ^{t}Bu 3, Ph 4)

2,2′-Bipyridine (bipy) (0.035 g, 0.22 mmol) was added to a pale yellow solution of **1** (0.1 g, 0.057 mmol) in 15 cm^3 of CH_2Cl_2 at r.t., to give a deep orange solution. After 5 min of stirring the solvent was removed under vacuum and treated with cold Et_2O ($\sim$5 cm^3) to give **3** as an orange solid. Yield: 87% (0.11 g).

Complex **4** was obtained as a yellow solid (yield 79%) by a similar procedure, using acetone as the solvent and **2** as the precursor.

Compound **3**: Anal. Calc. For $C_{44}H_{34}F_{10}N_4Cu_2Pt$: C, 46.73; H, 3.03. Found: C, 46.90; H, 2.91%. FAB^+ (selected data): 977 ($[M-bipy+3]^+$, 4). IR(cm^{-1}): 1934 s (C≡C), 808 s, 800 s $(C_6F_5)_{x\text{-sens}}$. ^1H-NMR (CD_3COCD_3): At 293 K, 10.04 (br, H33′, bipy), 8.63 (d, $J_{HH} = 7.9$, H66′, bipy), 8.31 (st, $J_{HH} \sim 7.3$, H55′, bipy), 7.82 (st, $J_{HH} \sim 5.4$, H44′, bipy), 0.76 (s, ^{t}Bu). By lowering the temperature, the resonance of the H33′ protons of the bipy decoalesces at ca. 223 K, splitting at 213 K (δ 11.65 and ca. 8.4). The signal at 8.4 overlaps with the resonance due to H55′ protons. ^{19}F-NMR (CD_3COCD_3): At 293 K, −115.4 (dm, $^3J_{PtF} = 386$, *o*-F), −167.6 (m, *m*-F), −168.26 (t, *p*-F). Although the *o*-F resonance broadens slightly as the temperature is lowered no decoalescence is observed in the lowest temperature limit (213 K). ^{13}C-NMR (CD_3COCD_3): At 293 K, 152.9, 152.8, 140.2, 127.0, 122.1 (s, bipy), 116.1 (br, C_β), 97.0 (br, C_α), 32.7 (s, $C(\underline{C}H_3)$), 31.6 (s, $\underline{C}(CH_3)$).

Compound **4**: Anal. Calc. For $C_{48}H_{26}F_{10}N_4Cu_2Pt$: C, 49.24; H, 2.24. Found: C, 49.38; H, 2.51%. FAB^+

(selected data): 1170 ([M]$^+$, 15). IR(cm^{-1}): 1930 s (C≡C), 800 s br (C_6F_5)$_x$-sens. ^{1}H-NMR (CD_3COCD_3): At 293 K, 9.82 (d, J_{HH} ~ 3, H33′, bipy), 8.44 (d, J_{HH} ~7.7, H66′, bipy), 8.21 (t, J_{HH} ~7.2, H55′, bipy), 7.74 (t, J_{HH} ~5.5, H44′, bipy), 7.02 (m, ArH, Ph). Upon cooling the bipy signals broaden, but only the resonance attributed to H33′ decoalesces at 223 K and clearly splits at 213 K (δ 11.75 and ca. 8.35). The signal at 8.35 overlaps with the broad resonance due to the H66′ protons. ^{19}F-NMR ($CDCl_3$): At 293 K, −115.91 (dm, $^3J_{PtF}$ = 383, *o*-F), −166.94 (m, *m*-F), −167.41 (t, *p*-F). Upon cooling the *o*-F and *m*-F signals broaden and finally the *o*-F resonance decoalesces at ca. 218 K and split at 213 K (δ at 213 K: −115.17, −116.96 (*o*-F), −165.05 (*m*-F), −165.41 (*p*-F)).

4.5. Preparation of [{cis-Pt(C_6F_5)$_2$(μ-C≡C^{t}Bu)$_2$}{Cu(dppe)}$_2$] (5)

Addition of 1,2-bis(diphenylphosphino)ethane (0.09 g, 0.23 mmol) to a yellow solution of **1** (0.1 g, 0.057 mmol) in CH_2Cl_2 (15 cm^3) immediately produced a colourless solution. Evaporation of the solvent and treatment of the residue with cold EtOH (~10 cm^3), afforded **5** as a white solid. Yield: 83% (0.15 g). Anal. Calc. For $C_{76}H_{66}F_{10}P_4Cu_2Pt$: C, 56.51; H, 4.12. Found: C, 56.22; H, 3.69%. FAB$^-$ (selected data): 1533 ([M−C$^t_2$Bu]$^+$, 7). IR(cm^{-1}): 2002 m, 1966 w (C≡C), 786 s, 778 s (C_6F_5)$_x$-sens. ^{1}H-NMR ($CDCl_3$): At 293 K, 7.28, 7.15 (ArH), 2.40 (s br, CH_2, dppe), 1.11 (s, ^{t}Bu). ^{19}F-NMR ($CDCl_3$): At 293 K, −114.45 (d, $^3J_{PtF}$ = 402, *o*-F), −168.25 (m, *m*-F), −168.87 (t, *p*-F). ^{31}P-NMR ($CDCl_3$): At 293 K, 6.55 (br).

4.6. Crystallography

Table 5 reports details of the structural analyses of all complexes. Pale-yellow crystals of complex **1** were obtained by slow diffusion of *n*-hexane into a solution of **1** in a mixture of acetone and Et_2O (5:1) at r.t. Crystals of complexes **2**·(acetone)$_4$ (yellow), **3** (orange) and **4** (yellow) were obtained by slow diffusion of *n*-hexane (**2**), Et_2O (**3**) or isopropylether (**4**) into acetone solutions of each compound at −30 °C. For all the complexes, data were collected as outlined in Table 5. No decay of the crystals was observed over the period of data collection.

For complexes **1**, **2**·(acetone)$_4$ and **3**, the cell parameters were obtained from ten frames using a 10° scan. Images were processed using the DENZO and SCALEPACK suite of programmes [26], carrying out the absorption correction at this point. For complex **4**, the cell constants were calculated from 50 reflections with 2θ angles ranging from 24 to 25°. An empirical absorption correction based on ψ-scans was applied, with maximum and minimum transmission factors being 0.997 and 0.717. The structures of **1** and **2**·(acetone)$_4$ were solved by Patterson and Fourier methods using the DIRDIF-92 programme [27], while the structure of **3** was solved by Direct Methods using the SHELXL-97 programme [28]. The three structures were refined by full-matrix least-squares on F^2 with SHELXL-97. The structure of **4** was solved by the Patterson method and refined by full-matrix least-squares on F^2 with SHELXL-93 [29]. For **1**, **3** and **4**, all non-hydrogen atoms were assigned anisotropic displacement parameters. In the case of **2**·(acetone)$_4$, all non-hydrogen atoms were assigned anisotropic displacement parameters, except the carbon and fluorine atoms of one C_6F_5 ligand (C(51)–C(56)), which were assigned isotropic parameters. This group presents a positional disorder, and could be refined over two positions with partial occupancy factors of 0.79/0.21. Additionally, the carbon atoms of the C_6F_5 group with lesser partial occupancy factors (C(51B)–C(56B)) were refined as an idealise aromatic ring, and the corresponding fluorine atoms (F(52B)–F(56B)) constrained to a distance of 1.35(0.01) Å from their respective carbon atoms. Also, two of the acetone ligands (those corresponding to O(1) and O(2)) present some disorder. In order to model these molecules, the O(1)–C(57) distance was constrained to 1.2(0.01) Å, while the methyl carbon atoms (C(58), C(59), C(61), C(62)) were constrained to a distance of 1.50(0.01) Å from the carbonyl carbon atoms. In all structures, the hydrogen atoms were constrained to idealised geometries and assigned isotropic displacement parameters 1.2 times the U_{iso} value of their attached carbon atoms (1.5 times for the methyl hydrogen atoms). Two of the structures possess solvent of crystallisation in the lattice. For complex **1** 3 molecules of water are found in the asymmetric unit, while for complex **4** there is a molecule of acetone in the asymmetric unit. In the case of complexes **2**·(acetone)$_4$ and **3**, residual peaks bigger than 1 e·Å^{-3} close to the heavy atoms have been observed, but with no chemical meaning.

5. Supplementary material

Crystallographic data for the structural analysis has been deposited with the Cambridge Crystallographic Data Centre, CCDC Nos.196866, 196867, 196868 and 196869 for **1**·3H_2O, **2**·(acetone)$_4$, **3** and **4**·acetone, respectively. Copies of this information may be obtained free of charge from The Director, CCDC, 12 Union Road, Cambridge CB2 1EZ, UK (Fax: +44-1223-336033; e-mail: deposit@ccdc.cam.ac.uk or www: http://www.ccdc.cam.ac.uk).

Table 5
Crystallographic data for **1**·3H_2O, **2**·(acetone)$_4$, **3** and **4**·acetone

	1·3H_2O	**2**·(acetone)$_4$	**3**	**4**·acetone
Empirical formula	$C_{54}H_{48}Cu_4F_{20}O_5Pt_2$	$C_{68}H_{44}Cu_4F_{20}O_4Pt_2$	$C_{44}H_{34}Cu_2F_{10}N_4Pt$	$C_{51}H_{32}Cu_2F_{10}N_4OPt$
Difractometer	Nonius KappaCCD	Nonius KappaCCD	Nonius KappaCCD	Siemens P4
Formula weight	1801.26	1949.37	1130.92	1228.98
Temperature (K)	173(1)	173(1)	293(2)	298(2)
Wavelength (Å)	0.71073	0.71073	0.71073	0.71073
Crystal system	Triclinic	Orthorhombic	Triclinic	Triclinic
Space group	$P\bar{1}$	*Pbca*	$P\bar{1}$	$P\bar{1}$
a (Å)	13.6723(1)	18.65600(10)	11.0500(10)	11.274(1)
b (Å)	13.6542(1)	21.0322(2)	11.9440(10)	14.279(1)
c (Å)	19.0476(2)	33.8166(3)	17.4830(10)	15.906(1)
α (°)	76.3652(4)	90	82.928(10)	94.09(1)
β (°)	69.5762(4)	90	80.492(10)	107.00(1)
γ (°)	89.8710(5)	90	68.605(10)	110.94(1)
V (Å^3)	3225.92	13268.85(19)	2113.9(3)	2242.2(3)
Z	2	8	2	2
D_{calc} (g cm^{-3})	1.854	1.952	1.777	1.820
Absorption coefficient (mm^{-1})	5.714	5.564	4.379	4.138
$F(000)$	1728	7488	1104	4009
Crystal size	0.20 × 0.15 × 0.3	0.50 × 0.50 × 0.45	0.45 × 0.35 × 0.20	0.50 × 0.32 × 0.20
Theta range for data collection (°)	4.18–26.37	4.10–27.10	4.09–30.50	2.03–25.00
Index ranges	$0 \le h \le 17$, $-17 \le k \le 17$, $-21 \le l \le 23$	$0 \le h \le 23$, $0 \le k \le 26$, $0 \le l \le 43$	$0 \le h \le 15$, $-15 \le k \le 16$, $-24 \le l \le 24$	$-12 \le h \le 1$, $-15 \le k \le 15$, $-18 \le l \le 18$
Reflections collected	15 361	16 892	12 655	8294
Independent reflections	13 100	14 555	12 655	7709
Data/restraints/parameters	13 100/0/782	14 555/11/863	12 655/0/556	7255/0/622
Goodness-of-fit on F^2	1.164	1.224	1.453	1.025
Final R indices [$I > 2\sigma(I)$]	$R_1 = 0.0314$, $wR_2 = 0.0787$	$R_1 = 0.0479$, $wR_2 = 0.1142$	$R_1 = 0.0345$, $wR_2 = 0.0970$	$R_1 = 0.0284$, $wR_2 = 0.0511$
R indices (all data)	$R_1 = 0.0626$; $wR_2 = 0.0848$	$R_1 = 0.0788$, $wR_2 = 0.1244$	$R_1 = 0.0370$, $wR_2 = 0.1019$	$R_1 = 0.0463$, $wR_2 = 0.0566$
Largest difference peak and hole (e Å^{-3})	0.944 and −0.622	1.728 and −1.014	1.189 and −2.337	0.526 and −0.412

Acknowledgements

We wish to thank the Dirección General de Investigación, Spain, and the Fondo Europeo de Desarrollo Regional (Projects BQU2002-03997-C02-01, 02-PGE-FEDER) and the Comunidad de La Rioja (APCI-2000/15) for their support of this research.

References

[1] Reviews: (a) R. Nast, Coord. Chem. Rev. 47 (1982) 89;
(b) W. Beck, B. Niemer, M. Wiesser, Angew. Chem. Int. Ed. Engl. 32 (1993) 923;
(c) J. Manna, K.D. John, H.-D. Hopkins, Adv. Organomet. Chem. 38 (1995) 79;
(d) J. Forniés, E. Lalinde, J. Chem. Soc. Dalton Trans. (1996) 2587;
(e) U. Rosenthal, P.M. Pellny, F.G. Kirchbauer, V.V. Burlakov, Acc. Chem. Res. 33 (2000) 119;
(f) U. Belluco, R. Bertani, R.A. Michelin, M. Mozzon, J. Organomet. Chem. 600 (2000) 37;
(g) D.M.P. Mingos, R. Vilar, D. Rais, J. Organomet. Chem. 641 (2002) 126.

[2] (a) I.R. Whittall, A.M. McDonagh, M.G. Humphrey, M. Samoc, Adv. Organomet. Chem. 42 (1998) 291;
(b) N.J. Long, Angew. Chem. Int. Ed. Engl. 34 (1995) 21.

[3] Reviews: (a) V.W.W. Yam, K.K.-W. Lo, K.M.-C. Wong, J. Organomet. Chem. 578 (1999) 3; (b) V.W.W. Yam, Acc. Chem. Res. 35 (2002) 555; (c) K.M.C. Wong, C.K. Hui, K.-L. Yu, V.W.W. Yam, Coord. Chem. Rev. 229 (2002) 123.

[4] (a) A. Harriman, R. Ziessel, J. Chem. Soc. Chem. Commun. (1996) 1707;
(b) P.F.H. Schwab, M.D. Levin, J. Michl, Chem. Rev. 99 (1999) 1863.

[5] (a) T.C. Higgs, P.J. Baiey, S. Parsons, P.A. Tasker, Angew. Chem. Int. Ed. Engl. 41 (2002) 3038 (and references therein);
(b) M.I. Bruce, B.C. Hall, B.W. Skelton, M.E. Smith, A.H. White, J. Chem. Soc. Dalton Trans. (2002) 995;
(c) J. Díez, M.P. Gamasa, J. Gimeno, E. Lastra, A. Aguirre, S. García Granda, Organometallics 16 (1997) 3684;
(d) K. Osakada, T. Takizawa, T. Yamamoto, Organometallics 14 (1995) 3531;
(e) D.L. Reger, J.E. Collins, M.F. Huff, Organometallics 14 (1995) 5457;
(f) D.M. Knotter, A.L. Spek, D.M. Grove, G. Van Koten, Organometallics 11 (1992) 4083;
(g) A.J. Edwards, M.A. Paver, P.R. Raithby, M.A. Rennie, C.A. Russell, D.S. Wright, Organometallics 13 (1994) 4967;
(h) F. Olbrich, J. Kopf, E. Weiss, Angew. Chem. Int. Ed. Engl. 32 (1993) 1077;
(i) F. Olbrich, U. Behrens, E. Weiss, J. Organomet. Chem. 472

(1994) 365;
(j) L. Naldini, F. Demartin, M. Manassero, M. Sansoni, G. Rassu, M.A. Zoroddu, J. Organomet. Chem. 279 (1985) C42;
(k) M.G.B. Drew, F.S. Esho, S.M. Nelson, J. Chem. Soc. Chem. Commun. (1982) 1347.

[6] (a) V.W.W. Yam, K.K.-W. Lo, W.K.-M. Fung, C.-R. Wang, Coord. Chem. Rev 171 (1998) 17;
(b) V.W.W. Yam, K.K.-W. Lo, Chem. Soc. Rev. 28 (1999) 323;
(c) J.P.H. Chartman, J. Forniés, J. Gómez, E. Lalinde, R.I. Merino, M.T. Moreno, A.G. Orpen, Organometallics 18 (1999) 353;
(d) H.B. Song, Q.M. Wang, Z.Z. Zhang, T.C.W. Mak, Chem. Commun. (2001) 1658;
(e) Y.G. Ma, W.-H. Chan, X.-M. Zhon, C.M. Che, New. J. Chem. (1999) 263;
(f) W.H. Chan, Z.Z. Zhang, T.C.W. Mak, C.M. Che, J. Organomet. Chem. 556 (1998) 169;
(g) J.H.K. Yip, J. Wu, K.Y. Wong, K.W. Yeung, J.J. Vittal, Organometallics 21 (2002) 1612;
(h) Y.Y. Lin, S.W. Lai, C.M. Che, K.K. Cheung, Z.Y. Zhon, Organometallics 21 (2002) 2275.

[7] Reviews: (a) P. Siemsen, R.C. Livingston, F. Diederich, Angew. Chem. Int. Ed. Engl. 39 (2000) 2632;
(b) K. Osakada, T. Yamamoto, Coord. Chem. Rev. 198 (2000) 379 and references therein;
(c) W. Carruther, in: G. Wilkinson, F.G.A. Stone, E.W. Abel (Eds.), Comprehensive Organometallics Chemistry, vol. 7, Pergamon, Oxford, 1982, pp. 722–724;
(d) B.H. Lipshutz, in: M. Sclosser (Ed.), Organometallics in Synthesys, Wiley, Chichester, 1995, pp. 300–302 and references therein;
(e) R.F. Heck, Palladium Reagents in Organic Synthesis, Academic Press, London, 1985, p. 299.

[8] (a) K. Osakada, R. Sakata, T. Yamamoto, Organometallics 16 (1997) 5354 and references therein; For some recent preparations see:
(b) J. Stahl, J.C. Bohling, E.B. Bauer, T.B. Peters, W. Mohr, J.M. Martín-Alvarez, F. Hampel, J.A. Gladysz, Angew. Chem. Int. Ed. Engl. 41 (2002) 1872.;
(c) M.S. Khan, M.R.A. Al-Mandhary, M.K. Al-Suti, N. Feeder, S. Nahar, A. Köhler, R.H. Friend, P.J. Wilson, P.R. Raithby, J. Chem. Soc. Dalton Trans. (2002) 2441;
(d) N.J. Long, A.J.P. White, D.J. Williams, M. Younus, J. Organomet. Chem. 649 (2002) 94;
(e) M.V. Russo, C. Lo Sterzo, P. Franceschini, G. Biagini, A. Furlani, J. Organomet. Chem. 619 (2001) 49.

[9] For some recent examples see: (a) V.W.W. Yam, K.L. Yu, K.M.C. Wong, K.K. Cheung, Organometallics 20 (2001) 721;
(b) S. Mihau, K. Sunkel, W. Beck, Chem. Eur. J. 5 (1999) 745;
(c) D. Rais, M.P. Mingos, R. Vilar, A.J.P. White, D.J. Williams, Organometallics 19 (2000) 5209;
(d) C.J. Adams, P.R. Raithby, J. Organomet. Chem. 578 (1999) 178.

[10] (a) H. Lang, K. Köhler, S. Blau, Coord. Chem. Rev. 143 (1995) 113;
(b) H. Lang, D.S.A. George, G. Rheinwald, Coord. Chem. Rev. 206–207 (2000) 101.

[11] (a) P. Espinet, J. Forniés, F. Martínez, M. Tomás, E. Lalinde, M.T. Moreno, A. Ruiz, A.J. Welch, J. Chem. Soc. Dalton Trans. (1990) 791;
(b) J. Forniés, M.A. Gómez-Saso, F. Martínez, E. Lalinde, M.T. Moreno, A.J. Welch, New J. Chem. 16 (1992) 483.

[12] J.C. Slater, J. Chem. Phys. 41 (1964) 3199.

[13] V.W.W. Yam, K.L. Yu, K.-K Cheung, J. Chem. Soc. Dalton Trans. (1999) 2913.

[14] S. Tanaka, T. Yoshida, T. Adachi, K. Onitsuka, K. Sonogashira, Chem. Lett. (1994) 877.

[15] I. Ara, J.R. Berenguer, E. Eguizábal, J. Forniés, E. Lalinde, A. Martín, Eur. J. Inorg. Chem. (2001) 1631.

[16] (a) P. Espinet, J. Forniés, F. Martínez, M. Sotés, E. Lalinde, M.T. Moreno, A. Ruiz, A.J. Welch, J. Organomet. Chem. 403 (1991) 253;
(b) J.R. Berenguer, E. Eguizábal, J. Forniés, E. Lalinde, A. Martín, F. Martínez, Organometallics 17 (1996) 4537.

[17] (a) I. Ara, J.R. Berenguer, E. Lalinde, M.T. Moreno, M. Tomás, J. Chem. Soc. Dalton Trans. (1995) 2397;
(b) J.R. Berenguer, J. Forniés, E. Lalinde, A. Martín, M.T. Moreno, J. Chem. Soc. Dalton Trans. (1994) 3343;
(c) I. Ara, J.R. Berenguer, J. Forniés, E. Lalinde, Inorg. Chim. Acta 264 (1997) 199;
(d) I. Ara, J.R. Berenguer, E. Eguizábal, J. Forniés, E. Lalinde, F. Martínez, Organometallics 18 (1999) 4344.

[18] D.L. Reger, J.E. Collins, M.F. Huff, A.L. Rheingold, G.A.P. Yap, Organometallics 14 (1995) 5475.

[19] M. Munakata, S. Kitagawa, I. Kawada, M. Maekawa, H. Shimono, J. Chem. Soc. Dalton Trans. (1992) 2225.

[20] J.A. Casares, P. Espinet, J.M. Martínez-Ilarduya, Y.-S. Lin, Organometallics 16 (1997) 770.

[21] I. Ara, J.R. Berenguer, E. Eguizábal, J. Forniés, J. Gómez, E. Lalinde, J.M. Sáez-Rocher, Organometallics 19 (2000) 4385 (and references therein).

[22] P.C. Ford, E. Cariati, J. Bourassa, Chem. Rev. 99 (1999) 3625.

[23] S. Braun, H.-O. Kalinowski, S. Berger, 100 and More Basic NMR Experiments, VCH, Weinheim, Germany, 1996.

[24] R.D. Stephens, C.E. Castro, J. Org. Chem. 28 (1963) 3313.

[25] R. Usón, J. Forniés, M. Tomás, B. Menjón, Organometallics 4 (1985) 1912.

[26] Z. Otwinowsky, W. Minor, Methods Enzymol. A: Macromol. Crystallogr. 276 (1997) 307.

[27] P.T. Beursken, G. Admiraal, G. Beursken, W.P. Bosman, S. García-Granda, R.O. Gould, J.M.M. Smits, C. Smykalla, The DIRDIF-92 Program System, Technical Report of the Crystallography Laboratory, University of Nijmegen, The Netherlands, 1992.

[28] G.M. Sheldrick, SHELXL-97, University of Göttingen, Göttingen, Germany, 1997.

[29] G.M. Sheldrick, SHELXL-93, FORTRAN-77 Program for Crystal Structure Determination from Diffraction Data, University of Göttingen, Göttingen, Germany, 1993.